

# Computational Contact Modelling of Hip Resurfacing Devices

Murat Ali and Ken Mao

**Abstract** A combination of computational models and theoretical methods have been used and developed to study the contact of hip resurfacing devices under normal and edge loading conditions. Techniques were developed and the solutions based on using the finite element method. It was found that the study of hip joint modelling, numerical methodologies of mechanical wear simulations and shakedown analysis can be developed to study the contact mechanics and biotribology of hip resurfacing devices under central and edge loading conditions. Each method developed in this study provides a unique platform to study these problems.

**Keywords** Biotribology · Contact · Finite element analysis · Microseparation · Shakedown · Wear

## 1 Introduction

Contact mechanics, wear and surface damage of hip resurfacing devices are subjects which have been studied since very early implantations and the longevity of the devices are becoming increasingly important. The wear and surface damage of these bearing surfaces occur through normal gait loading conditions, however, another problem is the stripe wear patterns observed on metal-on-metal patient retrievals [1] and assessed devices following hip simulator studies [2]. It has been claimed that edge loading occurs during the walking cycle of the patient; therefore ‘microseparation’ is simulated into each cycle during experimental wear testing [3]. The laxity of the hip joint is understood to lead to microseparation during the gait

---

M. Ali (✉) · K. Mao  
School of Engineering, University of Warwick, Coventry CV4 7AL, UK  
e-mail: murat.ali@warwick.ac.uk

K. Mao  
e-mail: k.mao@warwick.ac.uk

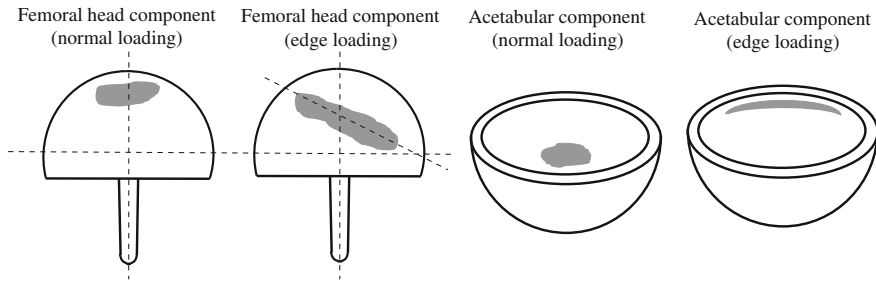


**Fig. 1** Hip resurfacing device with normal and edge loading wear patterns

cycle, and fluoroscopy studies have revealed how edge loading of the hip joint occurs due to lateral sliding of the femoral component during gait [3]. The differences between wear patterns observed during normal and edge loading conditions is shown schematically in Fig. 1. This study expands on the research conducted by Ali and Mao [4] to further develop techniques in assessing both the contact mechanics for wear modelling and the application shakedown theory to cyclically loaded hip resurfacing devices, particularly those under normal and microseparation conditions leading to edge loaded hip resurfaced bearings.

## 2 Contact, Wear and Shakedown Theory

Contact mechanics forms an integral part to predicting the contact stresses and mechanical wear associated with hip resurfacing devices. For studying the wear of orthopaedic devices, the Archard wear model [5] has been used with finite element analysis techniques. Although the Archard wear model [6] appears in many forms, the form most appropriate to be used within the finite element method has been described (1) where  $h$  is the linear wear depth,  $k_w$  is the dimensional wear coefficient,  $p$  is the contact pressure and  $s$  is the sliding distance.

$$h = k_w p s \quad (1)$$

Along with mechanical wear under cyclic contact, residual stresses can act to protect the component from plastic deformation by ensuring purely elastic material behaviour is reached in the longer term. Shakedown theory can be applied to assess the repetitive rolling and sliding contacts of elastic-perfectly plastic materials [7]. The transition from elastic to perfectly plastic occurs at the yield point of the stress-strain curve and this assumes that the material does not harden under loading conditions. Shakedown theory is based on Koiter's and Melan's theorems. Where Koiter's theorem defines the upper shakedown limit and kinematic shakedown theorem, and Melan's theorem provides the lower shakedown limit and static shakedown

theorem [8]. Under normal cyclic walking and edge loading of the hip joint, rolling and sliding contact is present. This is another indication that shakedown theory can be applicable to hip joints studies, as the theory was originally used to study rolling and sliding contact of elastic bodies. For the shakedown theory to be valid then plastic deformation must occur to initiate residual stresses leading to purely elastic steady state cycles, or in other words the yield strength must be exceeded for the residual stresses to be present following the load removal.

Edge loading has been assessed using experimental simulators under cyclic loading considering the rotation of the hip [9]. The significance of mild and severe microseparation conditions were shown, also in a separate study the kinematics and motions had a significant effect on the contact mechanics and wear rates of devices [10].

### 3 Methods and Materials

Computational and numerical methods have been used to investigate the mechanical contact of hip resurfacing devices under normal and edge loading conditions. A technique has been developed to take patient bone scans and build finite element (FE) contact models as described in Fig. 2. The acetabular cup and femoral head components were modelled using SolidWorks. These orthopaedic models were combined with pelvis and femur models in an assembly. The associative interface between the computer aided design model and finite element model allowed for geometrical modifications to be made to the orthopaedic devices. The analysis was conducted using ABAQUS (version 6.10-1) in combination with user defined subroutines and custom programming.

Common to all of the finite element models, the hip resurfacing device had a bearing diameter  $\varnothing_f$  of 50 mm and diametral clearance  $\varnothing_c$  of 80  $\mu\text{m}$  [11]. A simple contact model was used to carry out specific comparison studies, therefore the hip resurfacing components were backed and fully tied to rigid parts which were referred to as model 1 (shown in Fig. 3). The elasticity of attached bone was considered for the simulation of models 2–4. For initial conditions the cup and femoral head bearing centre's coincided, and all model boundary conditions were subsequently applied within specified time steps. The assembly of model 2 has been provided in Fig. 4.

A number of vertical loads were considered including: a 3900 N load which was based on the peak load  $F_y$  expected during the walking cycle and an ISO (International Organization of Standardization) load  $F_I$  of 3000 N. A stumbling load  $F_s$  of 11000 N was also applied as these high vertical loads have been highlighted to occur during patient stumbling [12]. For model 1 and model 2 the microseparation was modelled by translating the cup bearing centre in the lateral direction (i.e. along the anatomical lateral-medial axis) as used in experimental testing methods [9] and a finite element study of edge loading [13]. In addition to this method, 'pure' microseparation was also simulated, which more closely replicates the theoretical microseparation model proposed by Mak et al. [14].

**Fig. 2** Bone scans to FE contact models

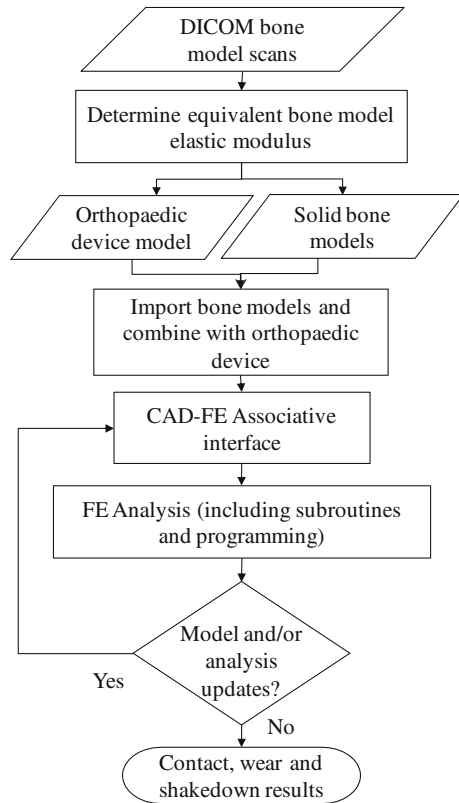
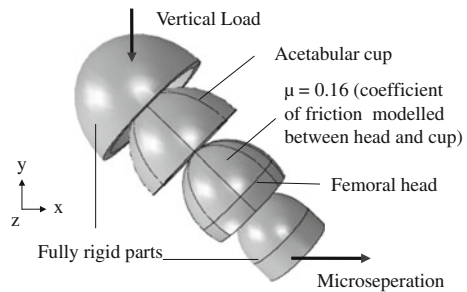
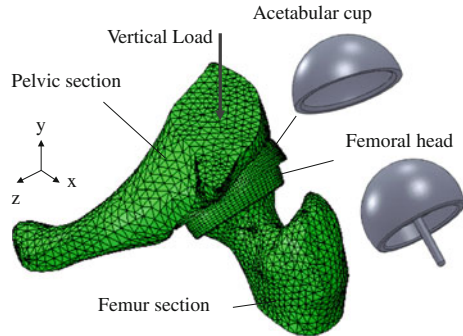


**Fig. 3** Assembly of rigid backed components (model 1)



The coefficient of friction ( $\mu$ ) between the head and cup was defined as 0.16 based on the friction factor of CoCrMo on CoCrMo (cobalt chromium molybdenum) in both bovine serum and synovial fluid [15]. The coefficient of friction value modelled in finite element analysis was shown to have a negligible effect on the contact stress [11], however, as the surface friction coefficient increases during the life of the component the subsurface stresses will also increase [16]. Therefore it has been considered in

**Fig. 4** Segmented hip model (model 2)



this study as the long term wear simulations can then take into account the increase in surface friction and surface roughness during the cyclic life of the component.

For this analysis, normal “Hard” contact behaviour was modelled and the material properties were obtained from literature and are summarised in Table 1 [17, 18]. For the application of shakedown theory, elastic-perfectly plastic ASTM F75 CoCrMo ‘as cast’ material properties were used [19]. For the bone model material an assessment was conducted to find an equivalent bone elastic modulus for the femur  $B_{EF}$  and pelvis  $B_{EP}$  to provide a simplified material model for the contact analysis. These values were determined by comparing the model stiffness of a CT (computed tomography) scanned femur and pelvis loaded in all three anatomical directions ( $x, y, z$ ) using the finite element method. A sensitivity analysis was carried out on the bone material model to compare the elastic modulus values between 3 and 25 GPa applied to the pelvis and femur.

A full hip finite element model (Fig. 5) were developed to provide validation for using a segmented model. Except for modelling the full femur and pelvic model, this geometrically matches that of the segmented model (model 2) for ease of comparison. By carrying out the finite element discretisation within the finite element analysis package meant that all the advanced tools within this environment could be utilized. A 2D axis symmetric model (Fig. 6) was developed following the techniques described by Udofia et al. [11] as a model to conduct a cyclic shakedown analysis and assess the subsurface stresses under different vertical loading conditions. Standard ISO loading and angular displacement data was used where flexion-extension and internal-external rotation was simulated for the wear analysis, which is where the majority of the sliding distance between the bearing devices would occur from.

**Table 1** Material properties

Material	Elastic modulus (GPa)	Poisson’s ratio	Density (kg/m <sup>3</sup> )
CrCoMo	230	0.3	8270
$B_{EF}$	12.3	0.3	1900
$B_{EP}$	6.1	0.3	1900

**Fig. 5** Full hip joint model (model 3)

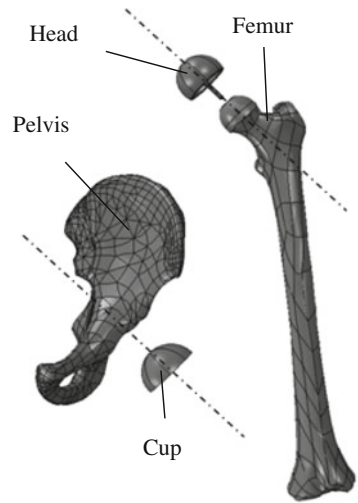
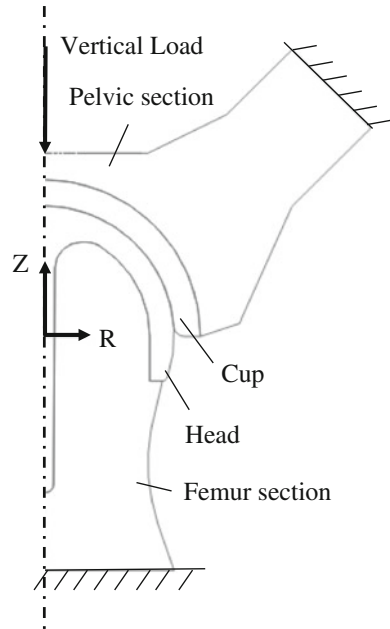


**Fig. 6** 2D Axis-symmetric model (model 4)



By studying the kinematics of the hip joint, it is claimed that microseparation occurs during the swing phase of gait [20, 21]. The swing phase occurs between 60 and 100% of the gait cycle, where the head and cup relocate fully during heel strike and edge loading occurs. As the frequency of the walking cycle ranges from 0.4–2.2Hz [22], it is expected that edge loading could occur over a time period of 0.5 s.

The wear simulations extract data from finite element analysis and the data was used to calculate the sliding distance and wear depth over a number of cycles. At predefined cyclic intervals the mesh is then updated without the need to use an adaptive meshing algorithm. For each identified number of cycles the total wear depth was calculated at each node on the bearing surface as shown in (2), where  $h_I$  is the total wear depth calculated over the total number of increments  $n$  for the analysis at each node of the bearing surface. The total volumetric wear over the testing period is given by  $h_T$  as shown in (3), where  $m$  is the total number of finite element mesh update increments. The dimensional wear coefficients are based on values provided in literature [23].

$$h_I = \sum_{i=1}^n kp_i(s_i - s_{i-1}) \quad (2)$$

$$h_T = \sum_{i=1}^m h_I \quad (3)$$

## 4 Results

For model 1 and based on the walking gait peak vertical load of 3900 N, the maximum contact stress was 101 MPa without consideration of microseparation. The contact pressure increased to a maximum of 1284 MPa along with 675 MPa von Mises stress when 250  $\mu\text{m}$  of lateral displacement was applied in combination with peak vertical loading conditions. By considering a lateral reaction force of 500 N (in line with experimental simulator test methods) without any vertical load led to a maximum contact stress of 564 MPa, von Mises stress of 456 MPa and maximum principal stress of 431 MPa. The simulation conducted on this model considered one cycle of edge loading and when the edge load was removed (i.e. contact removed) plastic strain was predicted to be less than 0.03 %. Through the assessment of edge loading due to ‘pure’ microseparation, the contact pressure between the head and cup again was predicted (Fig. 7). A symmetrical profile occurred about the centre of contact and the magnitude decreased as the distance from the centre of contact increased. The maximum contact stress did not occur directly on the rim radius of the cup, but above the rim radius. By using a spherical coordinate system to define the position of results, the contact stress magnitude decreased as the azimuthal angle  $\phi$  moved away from the centre of contact. All of the contact was observed below  $7^\circ$  of the polar angle  $\theta$ . By taking advantage of the customisable rigid backed model and through an efficient parametric study, the affect of cup inclination angle under ‘pure’ microseparation conditions have been observed (Fig. 8). The contact pressure increases as the cup inclination angle increased between 30 and 60°.

For model 2, a 250  $\mu\text{m}$  translation in the lateral direction led to an edge loading reaction force of 907 N. Based on the walking gait 3900 N peak vertical load the

**Fig. 7** Edge loading from 'pure' microseparation

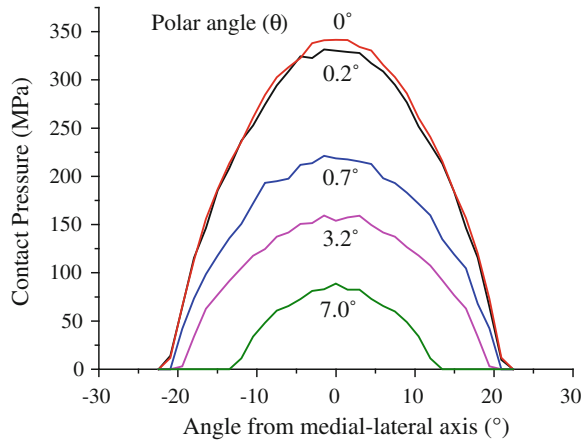
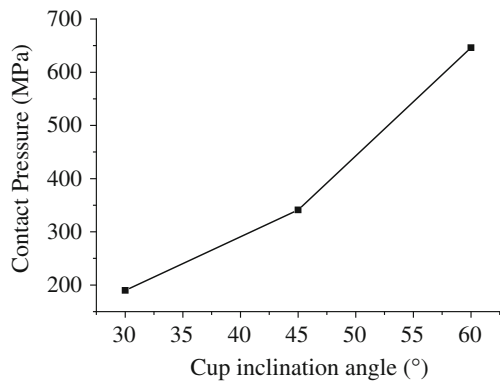


**Fig. 8** Variation of contact stress against cup inclination angle



maximum contact pressure was 18 MPa without consideration of microseparation (Fig. 9). The contact pressure and von Mises stress increased to a maximum of 142 and 141 MPa respectively when microseparation conditions were applied in combination with the peak vertical gait load (Fig. 10). When modelling an ISO gait loading profile in combination with a lateral sliding edge load the contact pressure profile is observed to be elliptical with the maximum contact pressure of 85 MPa occurring in the centre of contact.

The contact patch for edge loaded acetabular cups and femoral heads were noted to be elliptical (with a high  $b/a$  ratio) compared with a circular contact area during normal loading conditions. The total contact area for normal loading contact and edge loading contact is provided in Fig. 11, where the maximum contact area for normal loading ( $N_l$  and  $N_p$ ) and edge loading ( $M_l$  and  $M_p$ ) is highlighted.

By considering the affect of anteversion the segmented hip joint assembly was modified with a cup anteversion angle of  $15^\circ$ , the maximum contact stress occurred in the region where the cup was backed by a stiffer region of the pelvis. The results



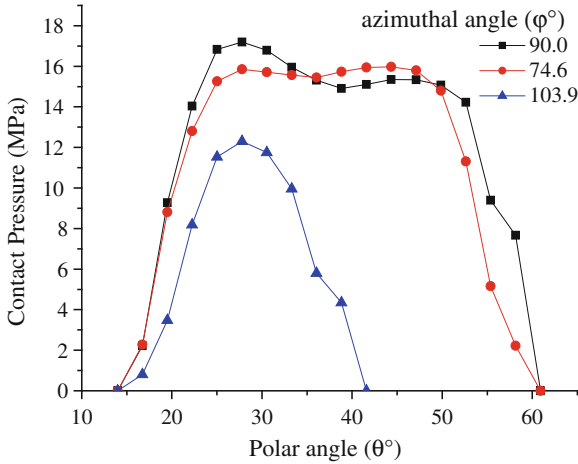


**Fig. 9** Contact pressure distribution during normal loading

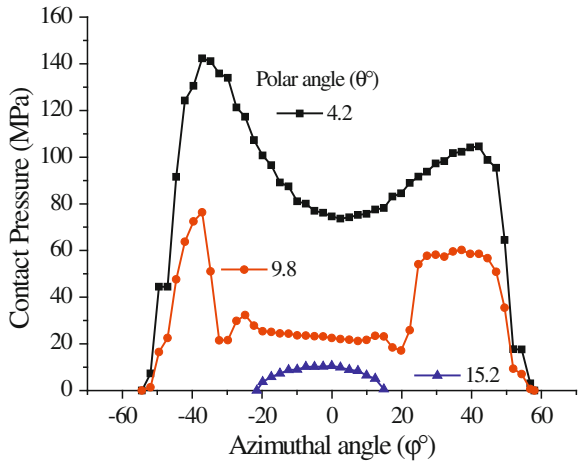


**Fig. 10** Contact pressure distribution during edge loading

obtained from the full hip model (model 3), showed maximum contact stress under normal loading conditions to be 17 MPa. The sensitivity analysis of bone material elasticity modulus is shown in Fig. 12.

Based on a representation of shakedown maps for line and circular contact [7, 24] and a friction coefficient of 0.16, the component will remain in an elastic state under contact loading as long as the load intensity  $P_o/k$  does not exceed 3 (Fig. 13), where  $P_o$  and  $k$  are the maximum contact stress and material shear yield strength respectively. Based on theoretical shakedown maps and considering the maximum contact stress observed, the load intensity of the hip resurfacing device  $P_o/k$  is predicted to

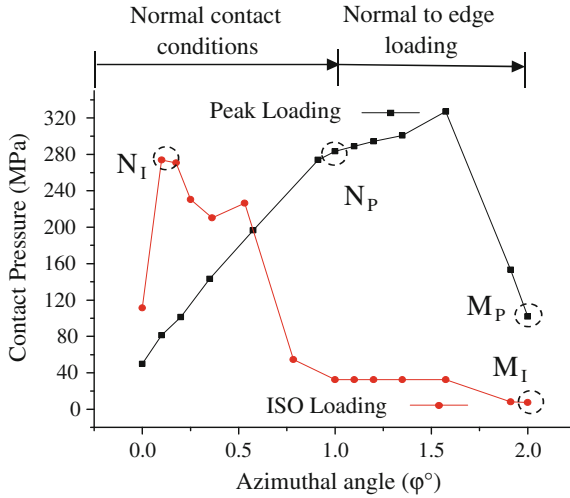


Fig. 11 Total contact area between the femoral head and acetabular cup

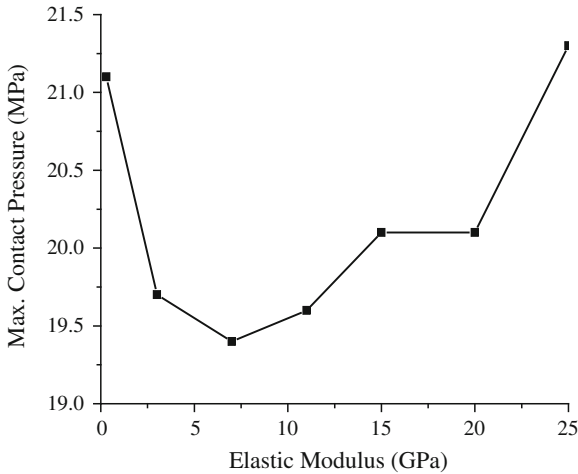
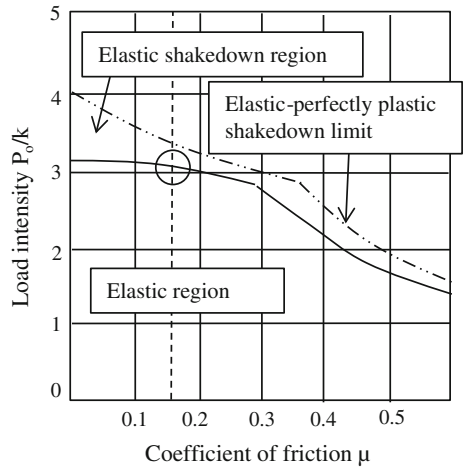


Fig. 12 Variation of contact pressure against bone elastic modulus

lie within the elastic region of the shakedown map and no elastic shakedown is predicted to occur. Following on from this result, by conducting the 2D axis-symmetric cyclic analysis using model 4, the stress-strain curve (Fig. 14) also predicted the hip resurfacing device material to remain within the elastic region under normal loading conditions even when high stumbling loads were considered.

The maximum von Mises stresses under the vertical loads  $F_I$ ,  $F_y$  and  $F_s$  are provided in Table 2. All the maximum von Mises stresses occurred below the surface of contact, it was only when a stumbling load  $F_s$  that the maximum von Mises

**Fig. 13** Shakedown map representation for line contact



**Fig. 14** 2D-Axis symmetric cyclic stress-strain curve during normal loading.

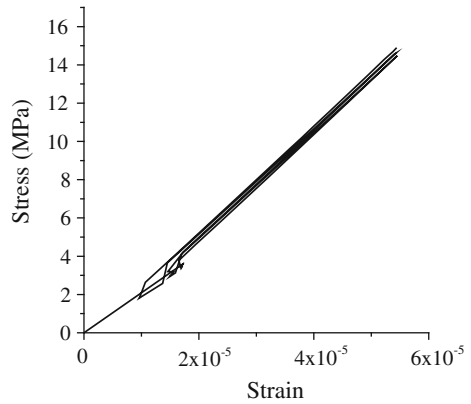


**Table 2** Maximum von Mises stress under vertical loads

Load	Acetabular cup (max. stress MPa)	Femoral head (max. stress MPa)
$F_l$	34	15
$F_y$	45	21
$F_s$	125	66 <sup>a</sup>

<sup>a</sup> 107 MPa predicted at the base of the femoral head stem

stress occurred at the at the bottom base of the head component. The mechanical wear prediction for the volumetric material loss due to mechanical wear of femoral head under flexion-extension rotation, internal-external rotation and ISO gait loading conditions was  $82 \text{ mm}^3/\text{mc}$  (per million cycles).

## 5 Discussion

By comparing the results obtained for all computational models the effect of bone elasticity on the contact stress and von Mises stress distributions were shown. Any asymmetrical contact and stress distributions were predicted to be caused by the unsymmetrical geometry of the human anatomy, but more importantly the vertical loading and microseparation conditions. When edge loading occurred through a lateral displacement of the femoral head with an ISO loading profile the contact pressure profile was symmetrical about the centre of contact. When modelling microseparation conditions, it was observed that the maximum contact pressure and von Mises stress occurred towards the anterior end of the acetabular cup and femoral head. For all three dimensional models, the plastic strains and stress were predicted to occur above the rim radius of the cup which matches the inspections from patient retrievals and bearing components following experimental simulator testing with microseparation. The corresponding contact profile on the femoral head component was also dependent upon the anteversion angle of the implanted cup. Due to the geometric nature of the femoral head, the anteversion of the cup would not have any effect upon the contact pressure profile and magnitude on the acetabular cup. The contact pressures were also found to be insensitive to bone elastic modulus, even though a large range of  $E$  values were modeled as a form of methodology verification.

The magnitude of stresses and contact pressures may appear large for model 1 however, the rigidity of backing components have shown to increase the results by at least a factor of 5 over the results obtained using models 2–4. These high levels of contact pressures and stresses have also been observed by Mak et al. [13]. The total contact area under edge loading conditions was at least 2.7 times less than under central or normal contact conditions. This is an important finding as the contact patch dimensions directly affects the linear wear as does the contact pressure according to the Archard wear model used to study wear of the bearing surfaces. Following on from the predictions and study of contact pressures, the mechanical wear simulations provided a numerical method for predicting the gravimetric volume loss of material following finite element ablation and comparing the total element volumes before and after the cyclic wear process. The results were dependent upon the specific boundary conditions, dimensional wear coefficient, contact pressure and sliding distance. The wear loss increased linearly which also agrees with linear wear observed from device tested using experimental simulators.

When considering both cyclic gait loading and high stumbling loads no plasticity was observed in models 2–4, therefore, in reality it is predicted that material plasticity is not predicted to occur under normal, edge loading or even extreme stumbling load conditions. Although no fatigue assessments were carried out in this study, it is an important consideration for any cyclically loaded component. Throughout this study it is deemed that fatigue strength along with fracture toughness of Cobalt Chromium Molybdenum are significantly larger than bone. The fracture toughness of CoCrMo is many times greater than for bone. This high fracture toughness would much sooner

cause femoral neck fracture, before fracture or fatigue failure of the metal-on-metal device.

The microseparation distance of  $250\ \mu\text{m}$  was equivalent to a force greater than that considered in experimental simulator studies which is typically  $200\text{--}500\ \text{N}$  in magnitude. It was possible to assess the reaction forces in the edge loaded regions to determine the contact stress results at specific loading magnitudes. This observation also explains the high values of edge loading contact stress observed in model 1. Based on the maximum contact pressure and calculated value of  $k$ , a low value of load intensity, suggests that the component under central and edge loading conditions would remain within the elastic region of a contact shakedown map, which is a 'safe' region for the component to be operating in under rolling and sliding contact. Therefore, in terms of the hip resurfacing devices response to loading, elastic shakedown, plastic shakedown or ratcheting behaviour is unlikely to be observed, during normal contact conditions, edge loading or stumbling load conditions.

By assessing affect of cup inclination angle under 'pure' microseparation and relocation, the increases in contact pressure above a  $45^\circ$  cup inclination agrees with the increased wear rates from patients with implanted hip resurfacing devices [25], however, it should be noted that this was conducted without any anteversion of the acetabular cup.

The mechanical wear simulations provided comparative results against the results obtained from experimental simulator studies considering the vast variation in methodologies and assumptions made between the numerical and experimental strategies.

## 6 Conclusion and Further Work

A combination of computational, numerical and theoretical techniques have been used and developed, which formed the basis of studying the contact mechanics, wear and shakedown of hip resurfacing device. The finite element method was used to build contact models, develop numerical mechanical wear techniques from previous studies and assess the application of shakedown theory to normal and edge loaded hip joint resurfacing devices under different loading conditions. The severity of edge loading contact was observed along with the significance and sensitivity of results based on the bone backed anatomical geometry and component assembly. From the assumptions made in this study and the modelling conditions to simulate normal and edge loading for hip joint resurfacing devices, predictions have shown that although cyclic loading is present during the operation of the hip resurfacing devices, elastic shakedown, plastic shakedown or ratcheting is not predicted to occur. The resurfacing device material is predicted to remain operating within the elastic region. It should be noted that this conclusion is drawn without the direct assessment of asperity shakedown, which will be considered in future studies.

The scope for studying the contact mechanics and wear of hip resurfacing devices within its designed applications of being implanted into patients is possible without

the need for complex density based material models. During this study it was found that an equivalent bone modulus can be used without the need for refinement as the affect on producing varied contact pressures was negligible.

The modelling of microseparation was carried out in two distinct and separate ways by applying both lateral sliding and ‘pure’ microseparation. Laxity of the joint is simulated based on a theoretical microseparation model which provides further explanation of the increasing wear rates observed by in-vitro studies and patient retrievals. Both microseparation simulation models showed an increase of contact pressure by at least a factor of 2 over normal or centrally loaded hip resurfacing devices depending on a number of factors, including the anteversion of the acetabular cup and loading conditions. This level of contact stress increase agrees with the level of wear rate increase from in-vitro experimental simulator studies of standard testing including microseparation.

The Archard wear model in combination with the FE solver, provided a basis for predicting the wear of the hip bearing surfaces. The methodological approach adopted in this study meant that numerical and process checks could be performed at every step to ensure that the developed simulations provided understandable results. Further work is required to reduce the cyclic block increments to update the finite element mesh more regularly, this will in turn allow for a contact pressure distribution which is dependant upon the worn surface geometry. The wear simulations should also consider the variation in dimensional wear coefficient throughout the cyclic life of the bearing components.

Modelling verification and comparative solutions to other studies and theoretical models have been developed for centered contact conditions; however, further work is required to develop theoretical and computational models to more accurately simulate and assess the effects of edge loading and microseparation on hip resurfacing devices. The kinematics of these conditions during human joint motion should be considered in more depth if simulations are to more accurately model these problems. Overall, using a combination of techniques and theoretical models has shown to be beneficial in developing the simulations to hip resurfacing devices under specific conditions.

**Acknowledgments** This work was fully supported and funded by the EPSRC (Engineering and Physical Sciences Research Council).

## References

1. Bowsher JG, Donaldson TK, Williams PA, Clarke IC (2008) Surface damage after multiple dislocations of a 38-mm-diameter, metal-on-metal hip prosthesis. *J Arthroplast* 23:1090–1096
2. Williams S, Stewart TD, Ingham E, Stone MH, Fisher J (2004) Metal-on-metal bearing wear with different swing phase loads. *J Biomed Mater Res Part B-Appl Biomater* 70B:233–239
3. Leslie IJ, Williams S, Isaac G, Ingham E, Fisher J (2009) High cup angle and microseparation increase the wear of hip surface replacements. *Clin Orthop Relat Res* 467:2259–2265
4. Ali M, Mao K (2012) Modelling of hip resurfacing device contact under central and edge loading conditions. In: *Lecture notes in engineering and computer science: Proceedings of the world congress on engineering 2012, WCE 2012*, 4–6 July. London, U.K, pp 2054–2059

5. Archard JF (1953) Contact and rubbing of flat surfaces. *J Appl Phys* 24:981–988
6. Maxian TA, Brown TD, Pedersen DR, Callaghan JJ (1996) A sliding-distance-coupled finite element formulation for polyethylene wear in total hip arthroplasty. *J Biomech* 29:687–692
7. Ponter ARS, Chen HF, Ciavarella M, Specchia G (2006) Shakedown analyses for rolling and sliding contact problems. *Int J Solids Struct* 43:4201–4219
8. Williams JA, Dyson IN, Kapoor A (Apr 1999) Repeated loading, residual stresses, shakedown, and tribology. *J Mater Res* 14:1548–1559
9. Stewart T, Tipper J, Streicher R, Ingham E, Fisher J (2001) Long-term wear of HIPed alumina on alumina bearings for THR under microseparation conditions. *J Mater Sci-Mater Med* 12:1053–1056
10. Firkins PJ, Tipper JL, Ingham E, Stone MH, Farrar R, Fisher J (2001) Influence of simulator kinematics on the wear of metal-on-metal hip prostheses. *Proc Inst Mech Eng Part H-J Eng Med* 215:119–121
11. Udofia IJ, Yew A, Jin ZM (2004) Contact mechanics analysis of metal-on-metal hip resurfacing prostheses. *Proc Inst Mech Eng Part H-J Eng Med* 218:293–305
12. Bergmann G, Graichen F, Rohlmann A, Bender A, Heinlein B, Duda GN et al (2010) Realistic loads for testing hip implants. *Bio-med Mater Eng* 20:65–75
13. Mak M, Jin Z, Fisher J, Stewart TD (2011) Influence of acetabular cup rim design on the contact stress during edge loading in ceramic-on-ceramic hip prostheses. *J Arthroplast* 26:131–136
14. Mak MM, Besong AA, Jin ZM, Fisher J (2002) Effect of microseparation on contact mechanics in ceramic-on-ceramic hip joint replacements. *Proc Inst Mech Eng Part H-J Eng Med* 216:403–408
15. Scholes SC, Unsworth A, Goldsmith AAJ (2000) A frictional study of total hip joint replacements. *Phys Med Biol* 45:3721–3735
16. Farley J (2008) Development of a computational method of low cycle fatigue prediction for multi-layer surfaces under rolling/sliding contact conditions. Ph.D. dissertation, School of Engineering and Design, Brunel University
17. Hodgskinson R, Currey JD (1992) Young modulus, density and material properties in cancellous bone over a large density range. *J Mater Sci-Mater in Med* 3:377–381
18. Dalstra M, Huijskes R, Vanerling L (1995) Development and validation of a 3-dimensional finite-element model of the pelvis bone. *J Biomech Eng-Trans Asme* 117:272–278
19. ASM International (2009) *Materials and coatings for medical devices: cardiovascular*. ASM International, Cleveland
20. Lombardi AV, Mallory TH, Dennis DA, Komistek RD, Fada RA, Northcut EJ (2000) An in vivo determination of total hip arthroplasty pistoning during activity. *J Arthroplast* 15:702–709
21. Dennis DA, Komistek RD, Northcut EJ, Ochoa JA, Ritchie A (2001) In vivo determination of hip joint separation and the forces generated due to impact loading conditions. *J Biomech* 34:623–629
22. Affatato S, Spinelli A, Zavalloni M, Mazzega-Fabbro C, Viceconti A (Dec 2008) Tribology and total hip joint replacement: current concepts in mechanical simulation. *Med Eng Phys* 30:1305–1317
23. Liu F, Leslie I, Williams S, Fisher J, Jin Z (2008) Development of computational wear simulation of metal-on-metal hip resurfacing replacements. *J Biomech* 41:686–694
24. Williams JA (2005) The influence of repeated loading, residual stresses and shakedown on the behaviour of tribological contacts. *Tribol Int* 38:786–797
25. Hart AJ, Buddhdev P, Winship P, Faria N, Powell JJ, Skinner JA (2008) Cup inclination angle of greater than 50 degrees increases whole blood concentrations of cobalt and chromium ions after metal-on-metal hip resurfacing. *Hip Int* 18:212–9